*Journal of Sound and Vibration* (1999) **221**(5), 805–821
*Article No*. jsvi.1998.1984, available online at http://www.idealibrary.com on IDEAL

# NON-LINEAR PARAMETER ESTIMATION USING VOLTERRA AND WIENER THEORIES

A. A. Khan and N. S. Vyas

*Department of Mechanical Engineering, Indian Institute of Technology, Kanpur, India*

(*Received* 16 *June* 1998, *and in final form* 14 *September* 1998)

This study explores the possibility of non-linear parameter estimation through use of Volterra and Wiener theories. An engineering approach is suggested by considering a single-degree-of-freedom system with cubic stiffness non-linearity. A third order kernel representation of the system response is taken. Using frequency domain analysis the first order and third order kernels are obtained. A third order kernel factor is synthesised from this first order kernel and is processed along with the third order kernel for estimation of the non-linear parameter. Damping is taken to be linear in the analysis. The procedure is illustrated through numerical simulation. The assumptions involved and the approximations are discussed. The influence of excitation force, linear damping parameter and probable measurement noise on the estimates is illustrated through non-dimensional simulation.



## 1. INTRODUCTION

Volterra and Wiener theories describe the relation between the output and the input in a functional form that cover a wide class of non-linearities. The application of these theories have so far been generally restricted to estimation of first and higher order kernels. Their structures, however, also offer rigorous theoretical platforms that can be explored for non-linear parameter identification.

Most of the commonly employed non-linear parameter estimation procedures work upon the first order frequency response function (FRF) and measure the distortion of the plot compared to one from the linear system. Otherwise, FRFs are taken repeatedly and the changes with different input levels are taken as measures of non-linearity.

Volterra [1] and Wiener [2] kernel theories provide the concepts of linear, bilinear, trilinear etc. kernels, which upon convolution with the excitation force and subsequent summation can be employed to represent the response of a non-linear system. Despite their attractive properties for analysis of non-linear physical systems, applications in relatively fewer situations [3–5] have been found for kernel estimation. The major reason behind this is the difficulty associated with the measurements of the kernels of the system and the enormous amount of

0022–460X/99/150805 + 17 $30.00/0 

computational effort required. French and Butz [6] simplified the computational problem significantly by suggesting the use of fast Fourier transforms in conjunction with a set of exponential functions as filters, instead of the orthogonal set of Laguerre functions used by Wiener or the alternative approach, suggested by Lee and Schetzen [7], of using cross-correlation techniques and time delay functions. Jahedi and Ahmadi [8] further applied the Wiener–Hermite expansion to non-stationary random vibration of a Duffing oscillator. Orabi and Ahmadi [9] have presented the non-stationary mean-square and autocorrelation responses of a Duffing oscillator using a truncated Wiener–Hermite series. Gifford and Tomlinson [10] have shown how a series of higher order FRFs, based on Volterra representation, provides a logical and appropriate way of extending linear system theory to cover non-linear systems. They illustrated correlation measurements for a non-linear beam under random excitation. Bendat [11] derived a range of formulae for calculation of linear, bilinear and trilinear Volterra response functions from measured input and output data and further [12, 13] illustrated their applications to non-linear systems.

The work cited above primarily deal with representation of the response of a non-linear system in terms of Volterra or equivalent Wiener kernels and estimation of the first and higher order kernels. However, numerical studies are scant and restricted to kernel estimation up to the second order. In the present work, an attempt has been made to extend the scope of these theories beyond kernel estimation, to the problem of extraction of the linear and non-linear parameters of the governing equation of the system. A single-degree-of-freedom system with cubic non-linearity in the stiffness term is considered. An engineering approach for parameter estimation is developed through a third order Volterra kernel representation of the system response. Damping is taken as linear in this analysis. Using frequency domain analysis, the first and third order kernels are extracted from measurements of the applied force and response. A third order kernel factor is synthesised from the first order kernel and is processed along with the third order kernel for estimation of the non-linear parameter. The procedure is illustrated through numerical simulation. The assumptions involved and the approximations are discussed. The influence of excitation force, linear damping parameter and probable measurement noise on the estimates is illustrated through non-dimensional simulation.

## 2. VOLTERRA SERIES REPRESENTATION OF RESPONSE

A system involving cubic non-linearity is considered

$$m\ddot{x} + c\dot{x} + kx + k_N x^3 = f(t), \tag{1}$$

where $m$ is the mass of the system considered, $k_N$ is the non-linear stiffness parameter to be estimated, while $c$ and $k$ are the unknown linear damping and stiffness terms. $f(t)$ in the above equation represents excitation given to the system.

The above equation is rewritten in non-dimensional form as

$$\eta''(\tau) + 2\xi\eta'(\tau) + \eta(\tau) + \lambda\eta^3(\tau) = \overline{f}(\tau), \tag{2}$$

where ($'$) denotes differentiation with respect to $\tau$, with $\tau = \omega_n t$ and

$$\omega_n = \sqrt{k/m}, \qquad \xi = c/2m\omega_n, \qquad \eta = x/x^*, \tag{3}$$
$$x^* = F_{max}/k, \qquad \lambda = k_N F_{max}^2/k^3, \qquad \overline{f}(\tau) = f(\tau)/F_{max}.$$

The system response, employing Volterra theory, is taken to be of the following form

$$\eta(\tau) = \mathbf{H}[\overline{f}(\tau)]$$
$$= \sum_{n=0}^{\infty} H_n[\overline{f}(\tau)], \tag{4}$$

where $H_n[\overline{f}(\tau)]$ is the $n$th order Volterra operator given by

$$H_n[\overline{f}(\tau)] = \int_{-\infty}^{\infty} \cdots \int_{-\infty}^{\infty} h_n(\tau_1, \ldots, \tau_n)\overline{f}(\tau - \tau_1) \cdots \overline{f}(\tau - \tau_n)\, \mathrm{d}\tau_1 \cdots \mathrm{d}\tau_n, \tag{5}$$

with the $n$th order Volterra kernel

$$h_n(\tau_1, \ldots \tau_n) = 0 \qquad \text{for } \tau_j < 0, \qquad j = 1, 2 \cdots n. \tag{6}$$

## 3. SYNTHESIS OF HIGHER ORDER VOLTERRA KERNEL FACTORS

The approach suggested by Schetzen [14] is employed, in which the Laplace transform of the first order kernel, $H_1(s)$ is first defined in terms of the linear parameters of the system, namely $\omega_n$ and $\xi$. The expressions for higher order kernel transforms $H_2(s)$, $H_3(s)$ etc. are consequently synthesised from the first order transform, $H_1(s)$, and the non-linear parameter $\lambda$.

Replacing the applied force $\overline{f}(\tau)$ by $c\overline{f}(\tau)$, the system response from equation (4) is

$$\sum_{n=1}^{\infty} c^n H_n[\overline{f}(\tau)] = \sum_{n=1}^{\infty} c^n \eta_n(\tau), \tag{7}$$

where, for convenience

$$\eta_n(\tau) = H_n[\overline{f}(\tau)]. \tag{8}$$

Substituting the new force and the response of equation (7) into equation (2) gives

$$\left\{\sum_{n=1}^{\infty} c^n \eta_n(\tau)\right\}'' + 2\xi\left\{\sum_{n=1}^{\infty} c^n \eta_n(\tau)\right\}' + \left\{\sum_{n=1}^{\infty} c^n \eta_n(\tau)\right\} + \lambda\left\{\sum_{n=1}^{\infty} c^n \eta_n(\tau)\right\}^3 = c\overline{f}(\tau). \tag{9}$$

The above power series representation of the governing equation is solved by equating the coefficients of like powers of $c$.

Equating the coefficients of the first power of $c$, one obtains

$$\eta_1''(\tau) + 2\xi\eta_1'(\tau) + \eta_1(\tau) = \overline{f}(\tau). \tag{10}$$

Noting from equation (4) that $\eta_1(\tau)$, the first term in the Volterra representation of $\eta(\tau)$, is the solution of the linear part of the differential equation (2), i.e.,

$$H_1[\overline{f}(\tau)] = \eta_1(\tau), \tag{11}$$

the Laplace transform of $H_1$ is

$$H_1(s) = 1/(s^2 + 2\xi s + 1). \tag{12}$$

Similarly, by equating the coefficients of $c^2$, one gets

$$\eta_2''(\tau) + 2\xi\eta_2'(\tau) + \eta_2(\tau) = 0. \tag{13}$$

The above requires the second order kernel $h_2$ to be identically zero, i.e.,

$$h_2(\tau_1, \tau_2) = 0. \tag{14}$$

By equating the coefficients of $c^3$, one gets

$$\eta_3''(\tau) + 2\xi\eta_3'(\tau) + \eta_3(\tau) = -\lambda\eta_1^3(\tau). \tag{15}$$

Similar to the case in equation (10), the above requires

$$\eta_3(\tau) = -\lambda H_1[\eta_1^3(\tau)]. \tag{16}$$

Since

$$\eta_3(\tau) = H_3[\overline{f}(\tau)], \tag{17}$$

one gets

$$H_3[\overline{f}(\tau)] = -\lambda H_1[\eta_1^3(\tau)], \tag{18}$$

and in terms of Laplace transforms,

$$H_3(s_1, s_2, s_3) = \lambda[\Psi(s_1, s_2, s_3)], \tag{19}$$

where the synthesised third order kernel factor, $\Psi(s_1, s_2, s_3)$, has been defined as

$$\Psi(s_1, s_2, s_3) = -H_1(s_1)H_1(s_2)H_1(s_3)H_1(s_1 + s_2 + s_3). \tag{20}$$

## 4. EXTRACTION OF WIENER KERNELS FROM RESPONSE

The two major problems, in the practical application of the Volterra series analysis, namely, measurement of individual Volterra kernels and convergence of the Volterra series, are circumvented through the use of Wiener functionals for

a stationary Gaussian white noise excitation $\overline{f}(\tau)$, with variance $A$. The Wiener kernel representation of this response is

$$\eta(\tau) = w_0 + \int_{-\infty}^{\infty} w_1(\tau_1)\overline{f}(\tau - \tau_1)\,\mathrm{d}\tau_1$$

$$+ \int_{-\infty}^{\infty}\int_{-\infty}^{\infty} w_2(\tau_1, \tau_2)\overline{f}(\tau - \tau_1)\overline{f}(\tau - \tau_2)\,\mathrm{d}\tau_1\,\mathrm{d}\tau_2 - A\int_{-\infty}^{\infty} w_2(\tau_1, \tau_1)\,\mathrm{d}\tau_1$$

$$+ \int_{-\infty}^{\infty}\int_{-\infty}^{\infty}\int_{-\infty}^{\infty} w_3(\tau_1, \tau_2, \tau_3)\overline{f}(\tau - \tau_1)\overline{f}(\tau - \tau_2)\overline{f}(\tau - \tau_3)\,\mathrm{d}\tau_1\,\mathrm{d}\tau_2\,\mathrm{d}\tau_3$$

$$- 3A\int_{-\infty}^{\infty}\int_{-\infty}^{\infty} w_3(\tau_1, \tau_1, \tau_2)\overline{f}(\tau - \tau_2)\,\mathrm{d}\tau_1\,\mathrm{d}\tau_2$$

$$+ \cdots, \tag{21}$$

whereby owing to the orthogonality property [2] between the Wiener and Volterra kernels, the individual kernels bear the following mutual relations (for a third order system response representation)

$$\begin{aligned} h_3(\tau_1, \tau_2, \tau_3) &= w_3(\tau_1, \tau_2, \tau_3), \qquad h_2(\tau_1, \tau_2) = w_2(\tau_1, \tau_2), \\ h_1(\tau_1) &= w_1(\tau_1) + w_{1(3)}(\tau_1), \qquad h_0 = w_0 + w_{0(2)}(\tau_1), \end{aligned} \tag{22}$$

with

$$w_{1(3)}(\tau_1) = -3A\int_{-\infty}^{\infty} w_3(\tau_1, \tau_2, \tau_2)\,\mathrm{d}\tau_2, \qquad w_{0(2)} = -A\int_{-\infty}^{\infty} w_2(\tau_1, \tau_1)\,\mathrm{d}\tau_1.$$

In view of the stated difficulties in the measurement of Volterra kernels, the measured system response is employed in the proposed parameter estimation algorithm, to extract the Wiener kernels. These Wiener kernels are then employed to generate the Volterra kernels, using the relationships of equations (22). The higher order "measured" Volterra kernels, thus obtained, are equated to those obtained from the synthesis procedure previously described for non-linear parameter estimation.

Extraction of Wiener kernels from measured response involves an enormous amount of data processing, since the kernels are multi-dimensional. The Laguerre filters proposed by Wiener [2] or the alternative approach, of using cross-correlation techniques and time delay filters [7] to perform the extraction, present formidable amounts of data processing. The use of a complex filter in the frequency domain [6] reduces the computational effort and is also suitable for such analysis since the Wiener kernel theory involves multidimensional convolutions. The scheme employing a complex exponential filter is shown in Figure 1(a).

Employing the Fourier transform representations

$$\bar{f}(\tau) = \int_{-\infty}^{\infty} \bar{F}(\omega)\, e^{j\omega\tau}\, d\omega, \qquad \eta(\tau) = \int_{-\infty}^{\infty} \eta(\omega)\, e^{j\omega\tau}\, d\omega,$$

$$w_1(\tau_1) = \int_{-\infty}^{\infty} W_1(\omega_1)\, e^{j\omega_1\tau_1}\, d\omega_1,$$

$$w_2(\tau_1, \tau_2) = \int_{-\infty}^{\infty}\int_{-\infty}^{\infty} W_2(\omega_1, \omega_2)\, e^{j(\omega_1\tau_1 + \omega_2\tau_2)}\, d\omega_1\, d\omega_2,$$

$$w_3(\tau_1, \tau_2, \tau_3) = \int_{-\infty}^{\infty}\int_{-\infty}^{\infty}\int_{-\infty}^{\infty} W_3(\omega_1, \omega_2, \omega_3)\, e^{j(\omega_1\tau_1 + \omega_2\tau_2 + \omega_3\tau_3)}\, d\omega_1\, d\omega_2\, d\omega_3, \quad (23)$$

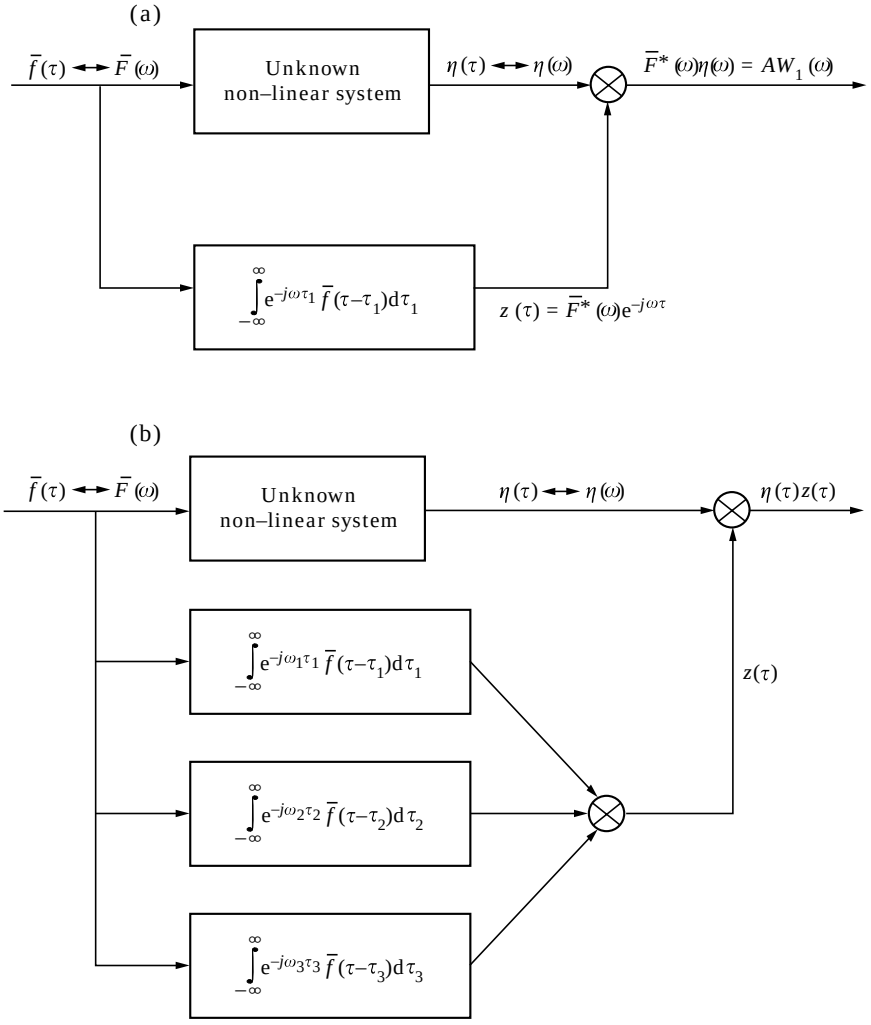


Figure 1. (a) Scheme for measurement of the first order kernel $W_1(\omega)$. (b) Scheme for measurement of the third order kernel $W_3(\omega, \omega, \omega)$.

equation (21) can be expressed as

$$\eta(\tau) = W_0 + \int_{-\infty}^{\infty} W_1(\omega_1)\bar{F}(\omega_1)\,\mathrm{e}^{j\omega_1\tau}\,\mathrm{d}\omega_1$$
$$+ \int_{-\infty}^{\infty}\int_{-\infty}^{\infty} W_2(\omega_1, \omega_2)\bar{F}(\omega_1)\bar{F}(\omega_2)\,\mathrm{e}^{j(\omega_1+\omega_2)\tau}\,\mathrm{d}\omega_1\,\mathrm{d}\omega_2$$
$$- A\int_{-\infty}^{\infty} W_2(\omega_2, -\omega_2)\,\mathrm{d}\omega_2$$
$$+ \int_{-\infty}^{\infty}\int_{-\infty}^{\infty}\int_{-\infty}^{\infty} W_3(\omega_1, \omega_2, \omega_3)\bar{F}(\omega_1)\bar{F}(\omega_2)\bar{F}(\omega_3)$$
$$\times\,\mathrm{e}^{j(\omega_1+\omega_2+\omega_3)\tau}\,\mathrm{d}\omega_1\,\mathrm{d}\omega_2\,\mathrm{d}\omega_3$$
$$- 3A\int_{-\infty}^{\infty}\int_{-\infty}^{\infty} W_3(\omega_1, \omega_2, -\omega_2)\bar{F}(\omega_1)\,\mathrm{d}\omega_1\,\mathrm{d}\omega_2 + \cdots. \tag{24}$$

The output $z(\tau)$, from the exponential filter is

$$z(\tau) = \int_{-\infty}^{\infty} \mathrm{e}^{j\omega\tau_1}\bar{f}(\tau-\tau_1)\,\mathrm{d}\tau_1$$
$$= \bar{F}^*(\omega)\,\mathrm{e}^{-j\omega\tau_1}, \tag{25}$$

where $\bar{F}^*(\omega)$ is the complex conjugate of $\bar{F}(\omega)$.

The ensemble average of the output of the circuit, Figure 1(a), is then obtained as

$$\langle\eta(\tau)z(\tau)\rangle = \langle\bar{F}^*(\omega)\rangle\,\mathrm{e}^{-j\omega\tau}W_0$$
$$+ \int_{-\infty}^{\infty} W_1(\omega_1)\langle\bar{F}(\omega_1)\bar{F}^*(\omega)\rangle\,\mathrm{e}^{-j\tau(\omega_1-\omega)}\,\mathrm{d}\omega_1$$
$$+ \int_{-\infty}^{\infty}\int_{-\infty}^{\infty} W_2(\omega_1, \omega_2)\langle\bar{F}(\omega_1)\bar{F}(\omega_2)\bar{F}^*(\omega)\rangle\mathrm{e}^{-j\tau(\omega_1+\omega_2-\omega)}\,\mathrm{d}\omega_1\,\mathrm{d}\omega_2$$
$$- A\langle\bar{F}^*(\omega)\rangle\,\mathrm{e}^{-j\omega\tau}\int_{-\infty}^{\infty} W_2(\omega_2, -\omega_2)\,\mathrm{d}\omega_2$$
$$+ \int_{-\infty}^{\infty}\int_{-\infty}^{\infty}\int_{-\infty}^{\infty} W_3(\omega_1, \omega_2, \omega_3)\langle\bar{F}(\omega_1)\bar{F}(\omega_2)\bar{F}(\omega_3)\bar{F}^*(\omega)\rangle$$
$$\times\,\mathrm{e}^{-j\tau(\omega_1+\omega_2+\omega_3-\omega)}\,\mathrm{d}\omega_1\,\mathrm{d}\omega_2\,\mathrm{d}\omega_3$$
$$- 3A\int_{-\infty}^{\infty}\int_{-\infty}^{\infty} W_3(\omega_1, \omega_2, -\omega_2)\langle\bar{F}(\omega_1)\bar{F}^*(\omega)\rangle\,\mathrm{e}^{-j\tau(\omega_1-\omega)}\,\mathrm{d}\omega_1\,\mathrm{d}\omega_2$$
$$+ \cdots. \tag{26}$$

For a stationary Gaussian white noise input $\overline{f}(\tau)$ with zero mean and variance $A$, the Fourier transform, $\overline{F}(\omega)$, is also a stationary Gaussian white noise process and the ensemble averages of the products transformed functions are, according to Raemer [15],

$$\begin{aligned}
\langle \overline{F}(\omega) \rangle &= 0 \\
\langle \overline{F}(\omega_1)\overline{F}(\omega_2) \rangle &= A\delta(\omega_1 + \omega_2) \\
\langle \overline{F}(\omega_1)\overline{F}(\omega_2)\overline{F}(\omega_3) \rangle &= 0 \\
\langle \overline{F}(\omega_1)\overline{F}(\omega_2)\overline{F}(\omega_3)\overline{F}(\omega_4) \rangle &= A^2[\delta(\omega_1 + \omega_2)\delta(\omega_3 + \omega_4)] \\
&\quad + A^2[\delta(\omega_1 + \omega_3)\delta(\omega_2 + \omega_4)] \\
&\quad + A^2[\delta(\omega_1 + \omega_4)\delta(\omega_2 + \omega_4)]. \qquad (27)
\end{aligned}$$

The relations of equation (27) reduce equation (26) to

$$\langle \eta(\tau)z(\tau) \rangle = AW_1(\omega). \qquad (28)$$

However, due to the equivalence of time and ensemble averages, the ensemble average $\langle \eta(\tau)z(\tau) \rangle$ can also be written as

$$\langle \eta(\tau)z(\tau) \rangle = \lim_{T\to\infty} \frac{1}{T} \int_{-T/2}^{T/2} \eta(\tau)z(\tau)\, \mathrm{d}\tau, \qquad (29)$$

giving

$$\langle \eta(\tau)z(\tau) \rangle = \overline{F}^*(\omega)\eta(\omega). \qquad (30)$$

Equations (28) and (30) give

$$AW_1(\omega) = \overline{F}^*(\omega)\eta(\omega),$$

from which the expression for the Fourier transform of the first order Wiener kernel is

$$W_1(\omega) = \overline{F}^*(\omega)\eta(\omega)/A. \qquad (31)$$

For measurement of the third order kernel, a circuit involving three exponential delay filters, as shown in Figure 1(b), is considered. The output, $z(\tau)$, from the exponential filters is

$$z(\tau) = \int_{-\infty}^{\infty} \mathrm{e}^{-j\omega_1\tau_1}\overline{f}(\tau - \tau_1)\, \mathrm{d}\tau_1 \int_{-\infty}^{\infty} \mathrm{e}^{-j\omega_2\tau_2}\overline{f}(\tau - \tau_2)\, \mathrm{d}\tau_2 \int_{-\infty}^{\infty} \mathrm{e}^{-j\omega_3\tau_3}\overline{f}(\tau - \tau_3)\, \mathrm{d}\tau_3. \qquad (32)$$

The above, after some algebraic manipulations, reduces to

$$z(\tau) = \bar{F}(-\omega_1)\bar{F}(-\omega_2)\bar{F}(-\omega_3)\, e^{-j(\omega_1+\omega_2+\omega_3)\tau}.$$

The ensemble average of the output of the circuit is now derived as

$$\begin{aligned}\langle \eta(\tau)z(\tau)\rangle = A^2[&W_1(\omega_1)\delta(-\omega_2-\omega_3)\, e^{j(-\omega_2-\omega_3)\tau} \\ &+ W_1(\omega_2)\delta(-\omega_1-\omega_3)\, e^{j(-\omega_1-\omega_3)\tau} \\ &+ W_1(\omega_3)\delta(-\omega_1-\omega_2)\, e^{j(-\omega_1-\omega_2)\tau}] + 6A^3W_3(\omega_1,\omega_2,\omega_3). \end{aligned} \tag{33}$$

The equivalence of time and ensemble averages gives

$$\langle \eta(\tau)z(\tau)\rangle = \lim_{T\to\infty}\frac{1}{T}\int_{-T/2}^{T/2}\eta(\tau)z(\tau)\,d\tau. \tag{34}$$

Equation (34) can be reduced to

$$\langle \eta(\tau)z(\tau)\rangle = \bar{F}(-\omega_1)\bar{F}(-\omega_2)\bar{F}(-\omega_3)\eta(\omega_1+\omega_2+\omega_3). \tag{35}$$

Equations (33) and (35) give the expression for the measurement of the Fourier transform of the third order Wiener Kernel as

$$\begin{aligned} W_3(\omega_1,\omega_2,\omega_3) = &(1/6A^3)[\bar{F}^*(\omega_1)\bar{F}^*(\omega_2)\bar{F}^*(\omega_3)\eta(\omega_1+\omega_2+\omega_3)] \\ &-(1/6A)[W_1(\omega_1)\delta(\omega_2+\omega_3) + W_1(\omega_2)\delta(\omega_1+\omega_3) \\ &+ W_1(\omega_3)\delta(\omega_1+\omega_2)]. \end{aligned} \tag{36}$$

$W_3(\omega_1,\omega_2,\omega_3)$ forms a multi-dimensional surface on the $(\omega_1,\omega_2,\omega_3)$ axes. Measurements are made for special trispectral kernels with $\omega_1=\omega_2=\omega_3=\omega$. These kernels are functions of only one variable $\omega$ and are much easier to compute and interpret. Bendat [11] has termed such single function transforms for Volterra series as Special Trispectral Kernel Transforms. The Special Trispectral Wiener Kernel Transform can be readily written from equation (36) as

$$W_3(\omega,\omega,\omega) = (1/6A^3)[\{\bar{F}^*(\omega)\}^3\eta(3\omega)] - (1/2A)[W_1(\omega)\delta(\omega)]. \tag{37}$$

## 5. PARAMETER ESTIMATION

The Special Trispectral Wiener Kernel Transforms can be extracted from the measurement of the applied random force and the system response and employing equations (31) and (37). Subsequently, for a third order representation of the system response, noting the equivalence between the Volterra and Wiener Kernels (equation (22)), the third order Special Trispectral Volterra Kernel Transform can be computed from

$$\begin{aligned} H_3(\omega,\omega,\omega) &= W_3(\omega,\omega,\omega) \\ &= (1/6A^3)[\{\bar{F}^*(\omega)\}^3\eta(3\omega)] - (1/2A)[W_1(\omega)\delta(\omega)]. \end{aligned} \tag{38}$$

Similarly, from the relations of equations (22), the expression for the first order Volterra kernel, in terms of the measured Wiener Kernels, becomes

$$H_1(\omega) = W_1(\omega) + W_{1(3)}(\omega), \tag{39}$$

where $W_1(\omega)$ is as given in equation (31) and $W_{1(3)}(\omega)$ is the first order derived kernel,

$$W_{1(3)}(\omega) = -3A \int_{-\infty}^{\infty} W_3(\omega, \omega_2, -\omega_2)\, \mathrm{d}\omega_2. \tag{40}$$

The linear parameters, $\omega_n$ and $\xi$ can be readily obtained by equating the measured first order Volterra kernel (of equation (39)) to its analytical expression given in equation (12). Standard curve fitting techniques can be used. These estimated linear parameters, $\omega_n$ and $\xi$, are employed further in the estimation of the non-linear parameter $\lambda$. The estimate for $\lambda$ is obtained by equating the synthesized expression (equation (19)) and the measured value (equation (38)) of the third order Volterra kernels of the system. Thus,

$$\lambda = \{(1/6A^3)[\{\overline{F}^*(\omega)\}^3 \eta(3\omega)] - (1/2A)[W_1(\omega)\delta(\omega)]\}/[\Psi(\omega, \omega, \omega)]. \tag{41}$$

The procedure is illustrated through numerical simulation of the response for the non-dimensional equation with cubic non-linearity, equation (2). Owing to the statistical nature of the estimation procedure, the response is simulated for various values of the non-linearity parameter, $\lambda$. This response is subsequently processed through the proposed procedure for estimation of parameters, including $\lambda$. The errors involved in the computational procedure are discussed by comparison between the estimated value of $\lambda$ and that used in the simulation of the response. (For an experimental study, it may also be useful to refer to an estimation procedure based on the exact probability density solution of the Duffing oscillator [16], to make an additional check on the estimates.) The procedure is also repeated for various values of the damping ratio, $\xi$.

The forcing function in the equation is the normalised random force, $\overline{f}(\tau)$, with zero mean value. The excitation force is simulated through random number generating subroutine and is normalised with respect to its maximum value $F_{max}$. The response is generated numerically for 4096 number of instances in the non-dimensional time ($\tau$) range 0–2048, using a standard fourth order Runge–Kutta subroutine. The response is computed from 2000 samples of the simulated random force. (The influence of the number of samples in the ensemble is discussed later.)

The power spectrum of the random force averaged over the ensemble of 2000 samples is shown in Figure 2(a). The corresponding ensemble average of the power spectrum of the response for non-linear parameter $\lambda = 0{\cdot}10$ and a damping ratio, $\xi = 0{\cdot}01$, can be seen in Figure 2(b). The first order Volterra kernel, $H_1(\omega)$, is then computed using the expression of equation (39) over the ensembles of the force and response (Figure 3(a)). The linear parameters $\omega_n$ and $\xi$ are computed from $H_1(\omega)$ through routine modal analysis procedures [17]. The linear parameters thus

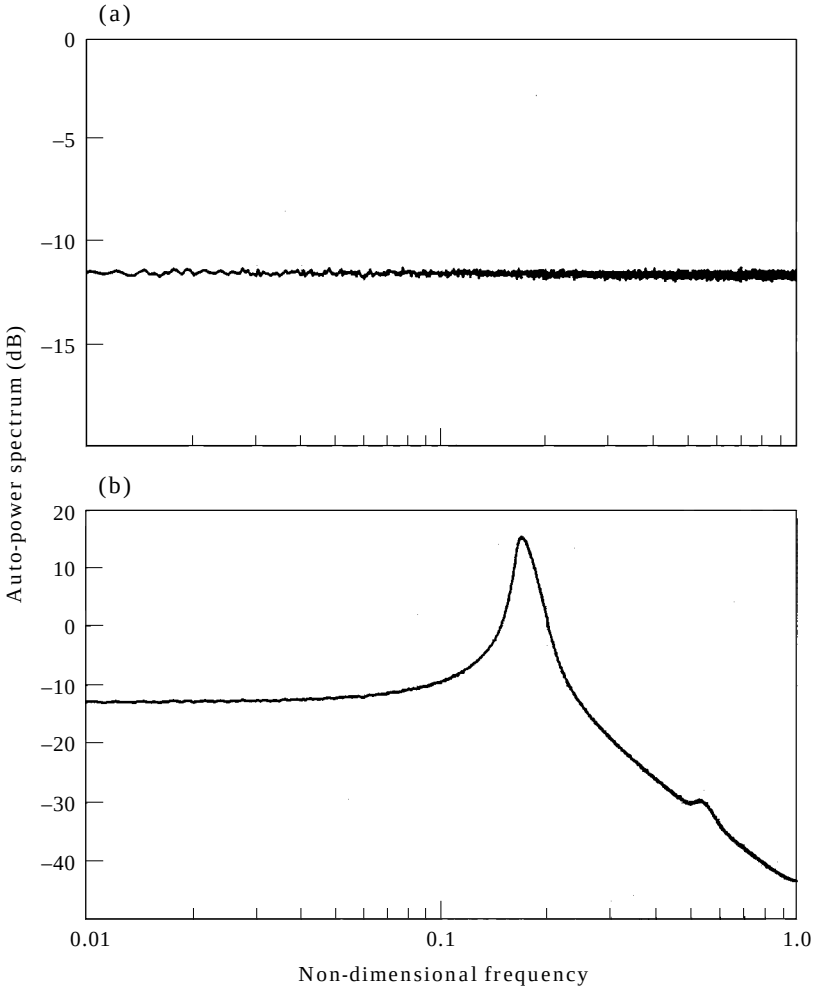


Figure 2. (a) Power spectrum of the input force. (b) Power spectrum of the response ($\lambda = 0{\cdot}1$; $\xi = 0{\cdot}01$).

estimated are $\omega_n = 1{\cdot}009$ (rad/non-dimensional time $\tau$) $= 0{\cdot}1606$ (cycles/non-dimensional time $\tau$) and $\xi = 0{\cdot}012$. The curve of Figure 3(b) shows the error incurred in the estimate of $H_1(\omega)$ due to the statistical nature of the Fast Fourier Transform computational procedure and the finite length of samples (4096 in the present case). The normalised random error can be seen to be at its maximum when it is in the vicinity of the natural frequency of the linear part of the system (1·0 rad/non-dimensional time $\tau$ i.e., 0·159 cycles/non-dimensional time $\tau$). For the ensemble size of 2000, the error in the frequency range 0·0–0·10 is less than 4%. It can be inferred that the normalised error for the higher order kernels would show a similar trend and the error, in the estimate of the non-linear parameter $\lambda$, can be expected to be less in the frequency zone 0·0–0·10.

The non-linear estimation is carried out for a range of values of the non-linear parameter $\lambda$ and damping ratios $\xi$. The response of the non-dimensional equation (2) is numerically simulated for $\lambda = 1{\cdot}00$, 0·10 and 0·01, while keeping the damping

ratio $\xi$ fixed at 0·01. It may be noted from equation (3) that the non-linear parameter $\lambda$ of the non-dimensional equation (2) includes both the nonlinear stiffness term $k_N$ and $F_{max}$, the maximum value of the applied force. A low value of $\lambda$ for a fixed value of $k_N$, implies a low value of $F_{max}$, while a high value of $\lambda$ for the same $k_N$, implies a high $F_{max}$ and vice versa. The results for such a non-dimensional parameter can be readily employed to design experiments and decide the excitation level for an expected non-linearity of a given system.

The estimated results for the third order kernel are depicted in Figure 4. The third order kernel factor $\Psi(\omega, \omega, \omega)$, synthesised from the measured first order kernel $H_1(\omega)$, and the measured third order kernel $W_3(\omega, \omega, \omega)$, are shown in Figure 4(a), (c) and (e) for $\lambda = 1{\cdot}00$, 0·1 and 0·01, respectively ($\xi = 0{\cdot}01$). It is to be noted here that while the first order kernel is estimated in the entire available frequency range 0·0–1·0, the third order kernels involving a $3\omega$ factor have to be restricted to one-third of this frequency zone (i.e., 0·0–0·33). It can be observed

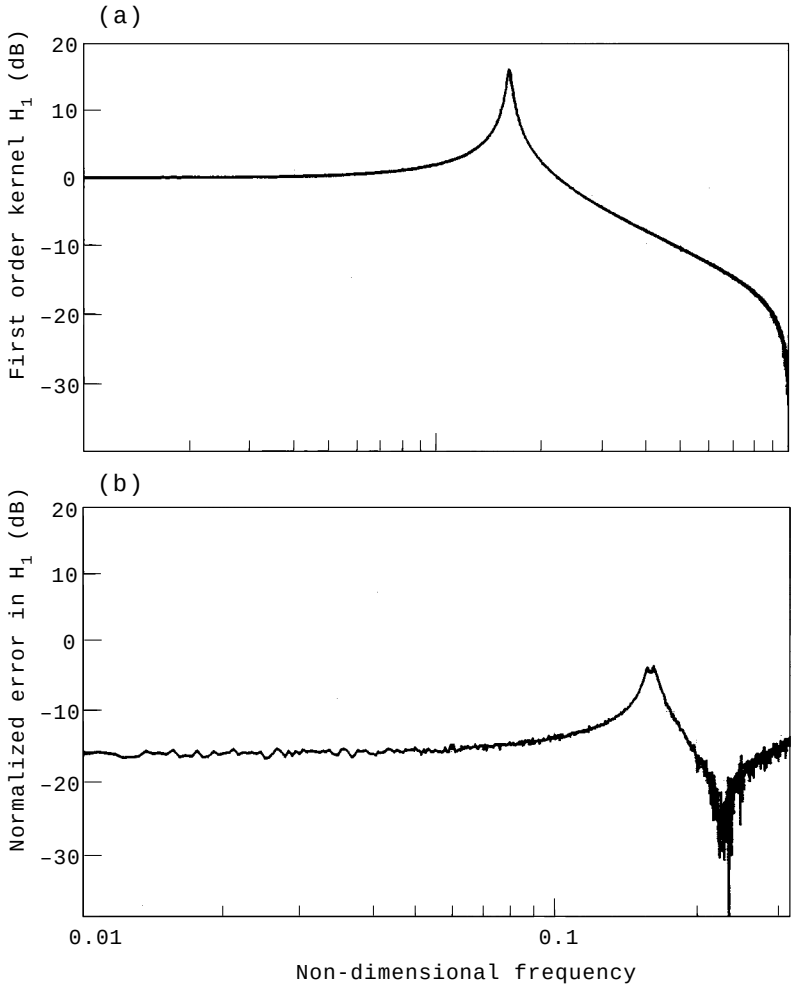


Figure 3. First order estimates ($\lambda = 0{\cdot}01$; $\xi = 0{\cdot}01$). (a) Estimate of $H_1$ ($\omega$); (b) Error in the estimate of $H_1$ ($\omega$).

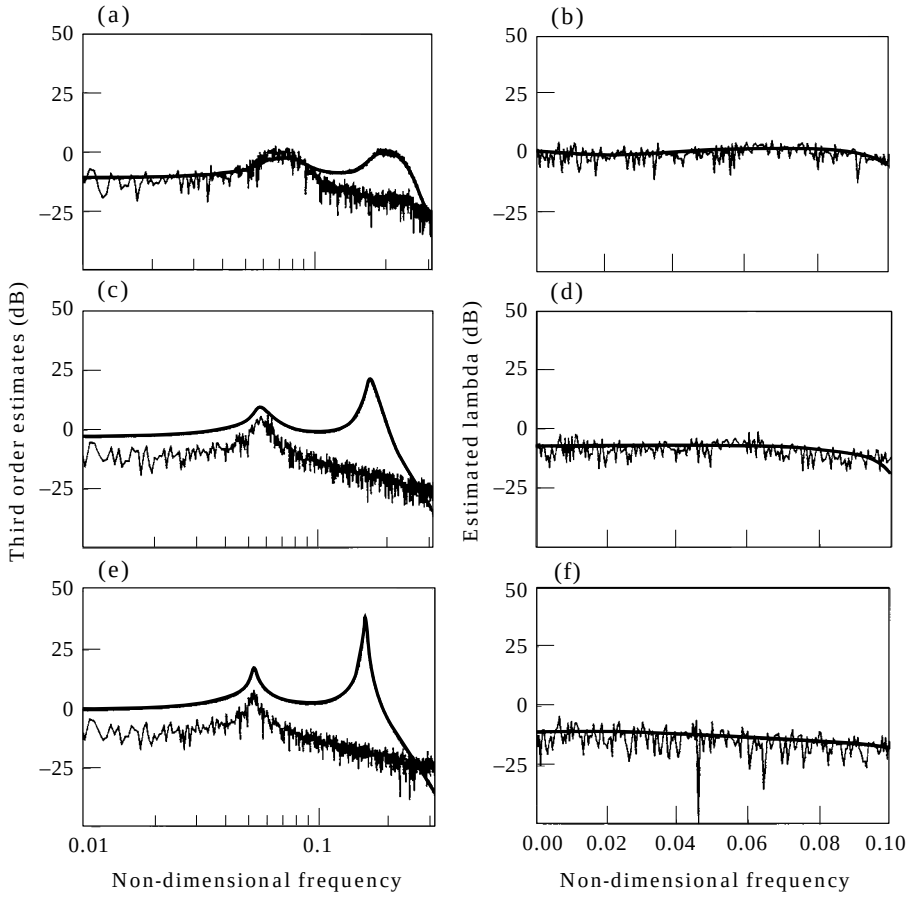


Figure 4. Estimates of third order kernels and non-linearity parameter $\lambda$ for various simulation values of $\lambda$ ($\xi = 0{\cdot}01$). Estimates of $\Psi(\omega, \omega, \omega)$ (——) and $W_3(\omega, \omega, \omega)$ (——) for simulation value of $\lambda = 1{\cdot}00$ (a), 0·10 (c) and 0·01 (e). Estimate of $\lambda$ for simulation value of $\lambda = 1{\cdot}00$ (b), 0·10 (d) and 0·01 (f).

from the figures that while the measured third order kernel $W_3(\omega, \omega, \omega)$ is reasonably accurate in showing the harmonic at $\omega_n/3$ (at non-dimensional frequency = 0·053), the identification of the harmonic at $\omega_n$ (at non-dimensional frequency = 0·159) is weak, the best approximation being in the case of $\lambda = 1{\cdot}0$. The estimation of $\lambda$ from these kernels is therefore restricted to the frequency zone of 0·0–0·1. The estimates of the non-linear parameter $\lambda$, obtained in accordance with the relationship (41), are shown in Figures 4(b), (d) and (f). A fourth order polynomial curve regressed through the estimates of $\lambda$, over the frequency range, is also shown in Figures 4(b), (d) and (f). The mean values of the estimates of $\lambda$ are found to be 1·08, 0·14 and 0·05, respectively. The order of the magnitude can be seen to be estimated correctly, while a good accuracy can be seen to be obtained for $\lambda = 1{\cdot}0$ (Figure 4(b)). It is to be noted here that the response representation of equation (24) has been restricted to include kernels only up to the third order, in order to keep the computations to a manageable level. Inclusion of higher order kernels (5th, 7th order) in the response representation can be expected to improve

the accuracy of the estimates with increased computational effort. Another source of inaccuracy in the estimates is the finite length of the samples and the ensemble size. The non-dimensional time interval for sampling has been taken as 0·5, and 4096 samples are collected for an ensemble for this numerical simulation which gives a frequency bandwidth of $\pm 1{\cdot}0$ cycles/non-dimensional time $\tau$ and a frequency resolution of $0{\cdot}488 \times 10^{-3}$ cycles/non-dimensional time $\tau$.

It was observed that increasing the sample size beyond 500 has insignificant influence on the first order estimates. The influence on the third order estimates can be seen from the curves of Figures 5(a)–(d). The figures show the power spectrum of the input for ensemble sizes 500, 1000, 1500 and 2000 along with the corresponding third order kernel function $\Psi(\omega, \omega, \omega)$ and the measured third order Wiener kernel, $W_3(\omega, \omega, \omega)$, which are both observed to become more refined with an increasing number of samples in the ensemble. In the present study the ensemble size has been limited to 2000. (It may also be noted that the numerical fourth order Runge–Kutta procedure of response simulation is also a source of error.)

Errors can be expected to be encountered during an experiment in the measurement of the excitation force and the response of a system as well. The influence of measurement noise is studied by contaminating the simulated force and response signals, with 5% simulated random noise. The frequency range is split into two and Figure 6(a) shows the third order kernel function $\Psi(\omega, \omega, \omega)$ and $W_3(\omega, \omega, \omega)$ for 5% noise in both input and output, in the frequency zone

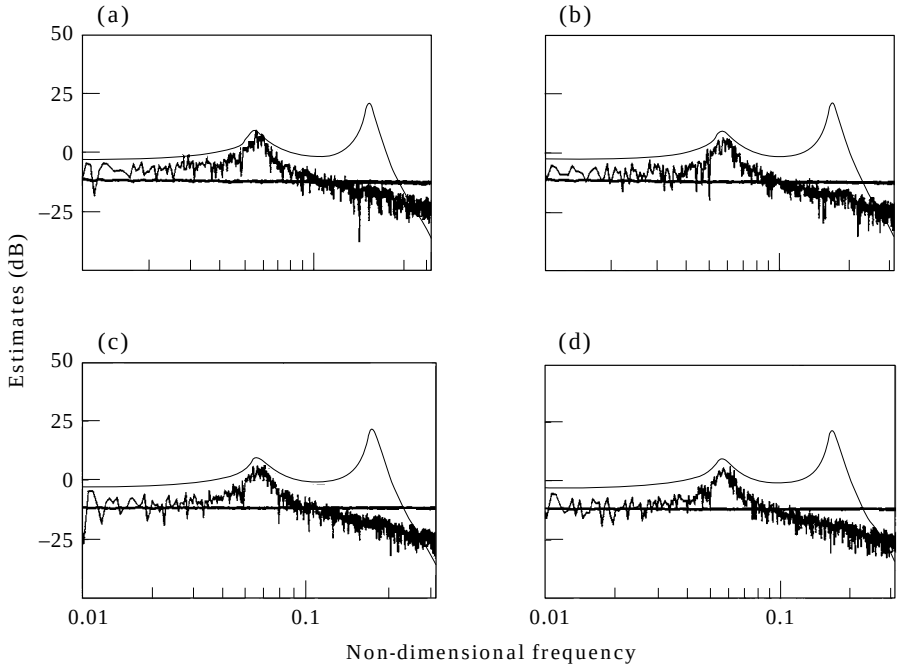


Figure 5. Influence of sample size on input auto-power spectrum and third order estimates (simulation values $\lambda = 0{\cdot}10$; $\xi = 0{\cdot}01$). Sample size = 500 (a), 1000 (b), 1500 (c) and 2000 (d). ~~~, Input power spectrum; —— measured Wiener kernel; ——, third order kernel factor.

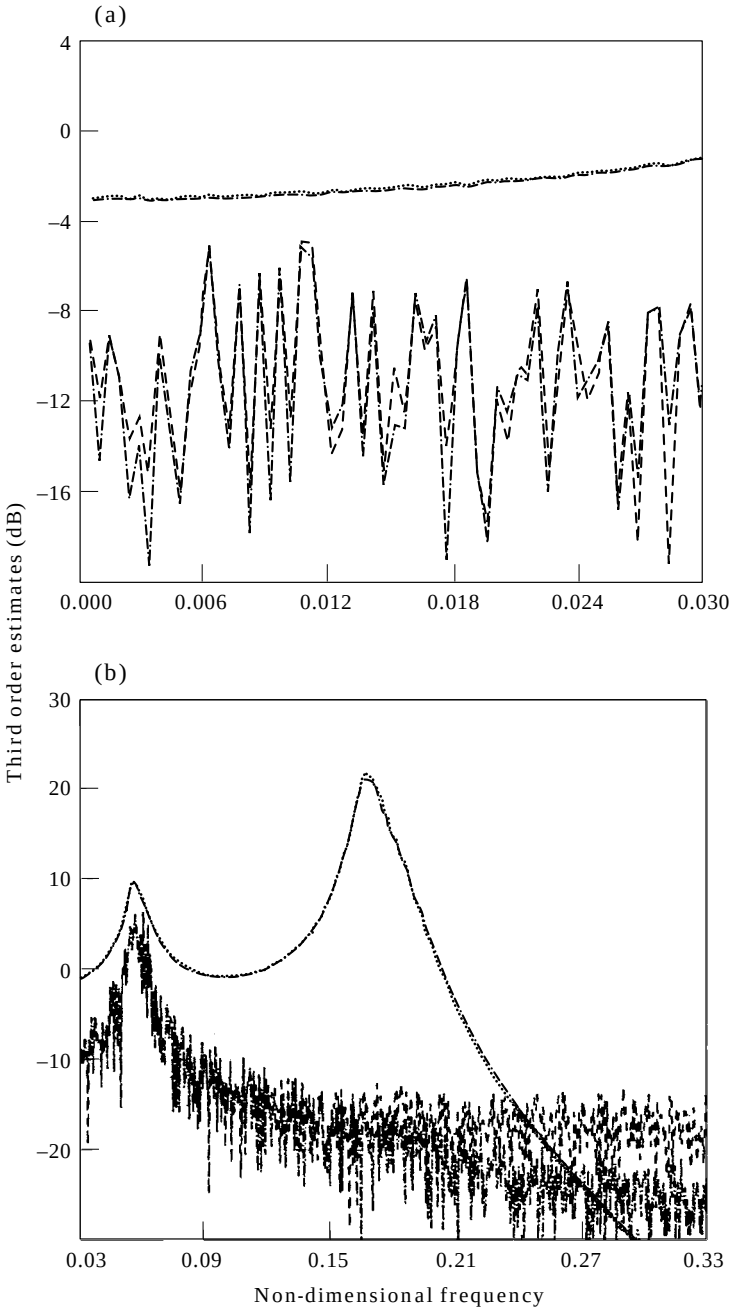


Figure 6. Effect of measurement noise on third order estimates (simulation values $\lambda = 0{\cdot}10$; $\xi = 0{\cdot}01$). $\Psi\ (\omega, \omega, \omega)$ and $W_3\ (\omega, \omega, \omega)$ in the frequency range of (a) 0·0–0·03 and (b) 0·03–0·33. ——, $w_3$ with 5% noise; · · · · · , $\Psi$ with 5% noise; ·–·–, $w_3$ with no noise; – – –, $\Psi$ with no noise.

of interest 0·00–0·03 on a magnified scale, while the remaining portions of the curves are shown in Figure 6(b). Other estimates are also observed to be similarly robust to measurement noise influence.

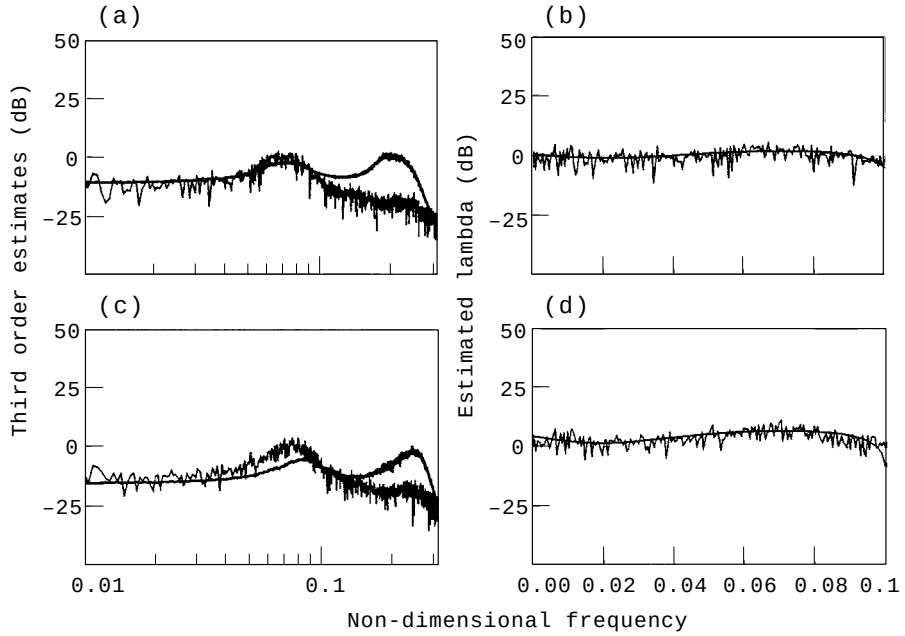


Figure 7. Influence of damping on third order and $\lambda$ estimates (simulation value of $\lambda = 1{\cdot}00$). Estimates of $\Psi\ (\omega, \omega, \omega)$ and $W_3\ (\omega, \omega, \omega)$ for simulation value of $\xi = 0{\cdot}01$ (a) and $0{\cdot}001$ (c). Estimate of $\lambda$ for simulation value of $\xi = 0{\cdot}01$ (b) and $0{\cdot}001$ (d).

Apart from the non-linear parameter $\lambda$, the other non-dimensional parameter contained by the governing equation (2) is the damping ratio $\xi$. Numerical simulation is carried out to check the validity of the estimation procedure for two different damping values. Figures 7(a)–(d) show the third order estimates and the estimated nonlinear parameter for damping values $\xi = 0{\cdot}01$ and $0{\cdot}001$ (for $\lambda = 1{\cdot}0$). The estimates can be seen to be sensitive to damping and for identical values of the non-linear parameter $\lambda$, the results are more accurate for higher damping.

## 6. REMARKS

The procedure developed gives good engineering estimates of the non-linear parameter. The estimates are satisfactory for a range of system damping. It also appears to be robust to measurement noise. The analysis presented is in non-dimensional form and can be suitably employed to design experiments. The accuracy of the estimates, as shown, is improved with the increase in the number of force and response samples over which averaging is carried out. The accuracy can be improved by involving kernels of orders higher than three and also by increasing the ensemble size. The increase in the computational effort may, however, need to be explored. Extension of the present procedures to systems with more than one degree of freedom and involving linear and non-linear coupling can be explored through incorporation of first and higher order cross-kernel concepts.

## ACKNOWLEDGMENT

The authors wish to express their thanks for the financial aid being provided by the Propulsion Panel of Aeronautical Research & Development Board, Ministry of Defence, Government of India, in carrying out the study.

## REFERENCES

1. V. Volterra 1958 *Theory of Functionals and of Integral and Integro-Differential Equations*. New York: Dover Publications, Inc.
2. N. Wiener 1958 *Nonlinear Problems in Random Theory*. New York: MIT and Wiley.
3. L. Stark 1969 *Automatica* **5**, 655–676. The pupillary control system: its nonlinear adaptive and stochastic engineering design characteristics.
4. J. Beatty 1971 Paper presented to the *Fourth Annual Winter Conference on Brain Research*, *Aspen*, *CO*. Measuring the Wiener kernels of CNS subsystems: a general method for systems analysis.
5. G. H. Harris and L. Lapidus 1967 *Industrial and Engineering Chemistry*. **59**, 66–81. The identification of nonlinear systems.
6. A. S. French and E. G. Butz 1973 *International Journal of Control* **17**, 529–539. Measuring the Wiener kernels of a nonlinear system using the Fast Fourier Transform Algorithm.
7. Y. W. Lee and M. Schetzen 1965 *International Journal of Control* **2**, 237–254. Measurement of Wiener kernels of nonlinear system by crosscorrelation.
8. A. Jahedi and G. Ahmadi 1983 *Journal of Applied Mechanics*, *Transactions of the ASME* **50**, 436–442. Application of Wiener–Hermite expansion to nonstationary random vibration of a Duffing oscillator.
9. I. I. Orabi and G. Ahmadi 1987 *International Journal of Nonlinear Mechanics* **22**, 451–465. A functional series expansion method for response analysis of nonlinear systems subjected to random excitations.
10. S. J. Gifford and G. R. Tomlinson 1989 *Journal of Sound and Vibration* **135**, 289–317. Recent advances in the application of functional series to nonlinear structures.
11. J. S. Bendat 1990 *Nonlinear System Analysis and Identification from Random Data*. New York: Wiley.
12. J. S. Bendat and A. G. Piersol 1993 *Engineering Applications of Correlation and Spectral Analysis*. New York: Wiley.
13. J. S. Bendat 1998 *Nonlinear System Techniques and Applications*. New York: Wiley.
14. M. Schetzen 1980 *The Volterra and Wiener Theories of Nonlinear Systems*. New York: Wiley.
15. H. R. Raemer 1969 *Statistical Communication Theory and Applications*. Englewood Cliffs, NJ: Prentice-Hall.
16. R. Tiwari and N. S. Vyas 1995 *Journal of Sound and Vibration* **187**, 229–239. Estimation of nonlinear stiffness parameters of rolling element bearings from random response of rotor bearing systems.
17. D. J. Ewins 1984 *Modal Testing*: *Theory and Practice*. Lectchworth, England: Research Studies Press.